Breakdown of statistical field theory of inhomogeneous polymers

Yohai Bar-Sinai and Eran Bouchbinder

Chemical Physics Department, Weizmann Institute of Science, Rehovot 7610001, Israel

The application of statistical field theory, where some physical quantities are assumed to depend only on long wavelength properties of macroscopic systems, is ubiquitous in many branches of physics. In many cases, however, it is difficult to directly test the validity of this assumption. Here we consider spatially inhomogeneous polymers undergoing Gaussian thermal fluctuations and calculate fluctuation-induced (Casimir-like) forces associated with free-energy variations with either properties of an inclusion (e.g. inhomogeneity formed by adsorbing molecules) or with external geometric constraints. Analytic results reveal qualitative discrepancies between the continuum and discrete theories for the former, but perfect agreement for the latter. This marks a breakdown of the continuum approach for inhomogeneous systems. Possible implications for fluctuation-induced entropic forces in a broader context are discussed.

Statistical Field Theory (SFT), bringing together continuum/field theory and statistical mechanics, is prevalent in the physical sciences [1–3]. The standard argument in favor of the continuum approach is that as many macroscopic variables of interest vary slowly in space, their statistical mechanics can be described by continuum field theories [4]. Thus, the continuum limit is taken, in some cases rigorously and in others less so, by coarse-graining discrete/miscroscopic variables into smoothly varying fields, and demanding that each field does not exhibit any variations on the scale of the constituent material elements [1].

When analyzing the *dynamics* of a given system, the choice of whether to use a discrete or a continuum approach is usually imposed by the relevant lengthscales under consideration. When analyzing the *thermodynamics* of a system, however, the calculation involves a thermal average over all modes of the system. Therefore, even when large lengthscales are considered, one cannot a priori exclude the possibility that the thermal average includes significant contributions from small lengthscale modes, for which the continuum approximation is invalid. Therefore, SFT can only be applied when thermal averages are dominated by long wavelength contributions.

In the last few decades SFT has been increasingly applied in the soft-matter and biophysics communities to a broad class of fluctuation-induced (Casimir-like) configurational forces. In this class of problems the free energy F of inhomogeneous systems is calculated based on a continuum-level energy functional. F depends on a set of variables $\mathbf{\Lambda} = \{\Lambda_1, \Lambda_2, \dots\}$ that break some symmetry of the system. The derivatives of the free energy with respect to these variables, $\partial F/\partial \Lambda_i$, are fluctuation-induced configurational forces. This approach was used to study numerous systems such as fluctuation-induced forces between membrane inclusions [5–7], rough surfaces [8, 9], colloids [10] and line defects [11]; membrane self-assembly [12], interactions and correlations in liquid crystals [13], and other phenomena [3, 14–16].

It may be argued that although the free energy F is not dominated by long wavelength contributions, the continuum calculation of fluctuation-induced configurational (entropic) forces is nonetheless valid since the *variation* of F upon changes in Λ_i depends only on long wavelengths. That is, one may hypothesize that changing Λ_i affects mainly the long wavelength normal modes, or at least that the variation of the contribution of short wavelength modes somehow cancels out. While this is possible, to the best of our knowledge such a claim has not been substantiated in the literature by considering the corresponding discrete theory (DT).

Facing this concern, we analyze in this Letter a relatively simple member of this broad class of problems: a spatially inhomogeneous polymer chain undergoing overdamped Gaussian thermal fluctuations in a surrounding solvent. For this system the discrete theory (DT) and the statistical field theory (SFT) may be fully tractable analytically, allowing a quantitative comparison between the two theories. Our analytic results reveal fundamental discrepancies in some fluctuation-induced forces associated with the inhomogeneity, which is our main result.

We consider a spatially inhomogeneous one-dimensional polymer of length L, consisting of N monomeric units, submerged in a solvent of temperature T (cf. Fig. 1). $x \in [0, L]$ is the coordinate along the polymer. To keep the discussion as elementary as possible, we study gradient driven dynamics, physically corresponding to torsional or extensional/stretching deformations. Similar results can be obtained for more complicated dynamics, such as bending deformations. The polymer is assumed to be bounded by a wall whose position is externally controlled, constraining the possible configurations of the polymer.

A key point is that the polymer is *spatially inhomogeneous*, i.e. its linear elastic moduli are space-dependent. There are many physical systems that might give rise to such a situation. For example, actin filaments in cells are known to significantly soften in regions where cofilin molecules bind to them [17–20], so partially cofilin-decorated actin filaments are spatially inhomogeneous. Other natural (e.g. biopolymers, such as partially histone-bound DNA, and hetero-proteins) and manmade systems can exhibit similar spatial inhomogeneity. Our discussion, however, remains general, independently of the details of the underlying physical system.
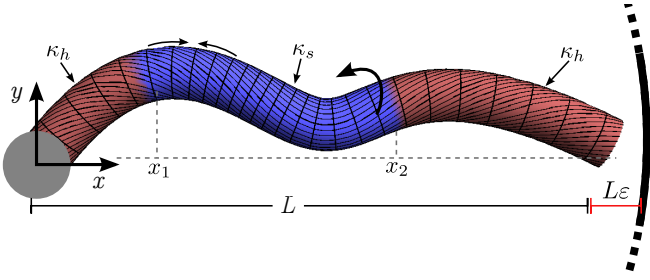
For concreteness, we consider a polymer composed of

FIG. 1. A fluctuating inhomogeneous polymer of length L, constrained within a sphere radius $L(1+\varepsilon)$ (a section of which is shown). One end of the polymer is fixed at the origin. A soft inclusion with rigidity κ_s, smaller than a background rigidity κ_h, extends from x_1 to x_2. Bending, stretching and torsional fluctuations are schematically shown.

3 locally homogeneous regions with sharp interfaces between them. That is, we consider an inclusion inside a polymer, as shown in Fig. 1, such that the elastic modulus is space-dependent; it equals κ_s inside the inclusion (for $x \in [x_1, x_2]$) and κ_h otherwise. The subscripts h, s denote "hard" and "soft", respectively. In addition, the fluctuations are bounded by a global constraint, say a sphere of radius $L(1 + \varepsilon)$. The symmetry-breaking parameters are $\mathbf{\Lambda} = \{\phi, \Delta, \varepsilon\}$, where are $\phi \equiv (x_2 - x_1)/L$ is the fraction of the soft part and $\Delta \equiv \sqrt{\kappa_h/\kappa_s}$ is a dimensionless measure of the rigidity contrast. Note that $0 \le \phi \le 1$ and $\Delta \ge 1$.

When the inhomogeneous polymer is submerged in an equilibrium solvent, it undergoes overdamped fluctuations characterized by deviations $w(x)$ from a reference rest state. The continuum elastic energy functional associated with these fluctuations is

$$U^{\mathrm{SFT}} = \tfrac{1}{2} \int_0^L \kappa(x) \left[w'(x) \right]^2 dx , \qquad (1)$$

where a prime denotes spatial differentiation. Once boundary conditions are specified, say $w(0) = w'(L) = 0$ (corresponding to one fixed and one free edges), the problem is fully defined. None of the results to follow depend qualitatively on the type of boundary conditions imposed.

The very same problem can be formulated at the discrete level, making reference to monomeric degrees of freedom and lengthscales. In particular, the discrete theory (DT) energy functional takes the form

$$U^{\mathrm{DT}} = \tfrac{1}{2} \sum_{i=1}^{N+1} \kappa_i \left(\frac{w_i - w_{i-1}}{\Delta x} \right)^2 \Delta x , \qquad (2)$$

where $\Delta x \equiv L/N$ is a monomeric lengthscale, κ_i, w_i are the discrete version of $\kappa(x)$ and $w(x)$, respectively, and i is the monomer index. The boundary conditions read $w_0 = \kappa_{N+1} = 0$.

Equations (1)-(2) are representative of a large class of physical systems whose energy functionals, in the

quadratic approximation, can be written as

$$U^{\mathrm{SFT}} = \tfrac{1}{2} \langle w(x) | \mathfrak{L} | w(x) \rangle = \frac{1}{2L} \int_0^L w(x) \, \mathfrak{L} \, w(x) \, dx , \quad (3)$$

$$U^{\mathrm{DT}} = \tfrac{1}{2} \langle \boldsymbol{w} | \boldsymbol{H} | \boldsymbol{w} \rangle = \tfrac{1}{2} \sum_{i,j} w_i H_{ij} w_j , \qquad (4)$$

where $\boldsymbol{H}$ is a real symmetric positive definite matrix (the Hessian, or Hamiltonian, matrix) and $\mathfrak{L}$ is a self-adjoint real differential operator [21]. In what follows, in order to emphasize the similarity between the discrete and continuum calculations we will denote the dynamic operator by $\mathfrak{D}$, which would correspond either to $\boldsymbol{H}$ or to $\mathfrak{L}$, depending on the context. Our convention is that the eigenvalues of $\mathfrak{D}$ are of energy dimensions, and accordingly the variables w_i and $w(x)$ are dimensionless. Equations (1)-(2) are recovered from Eqs. (3)-(4) when one identifies $\mathfrak{L}\{w\} = -L \left(\kappa(x) w'(x) \right)'$ and $\boldsymbol{H} = \boldsymbol{\nabla}\boldsymbol{\nabla} U^{\mathrm{DT}}$. The same framework, of course, describes other physical situations such as bending fluctuations, where w represents the deflection and the quadratic elastic energy density is controlled by curvature, i.e. $U = \tfrac{1}{2} \int \kappa(x) [w''(x)]^2 dx$.

Since we consider quadratic systems, the partition function Z involves Gaussian integrals. There are two distinct ways by which the constraints $\mathbf{\Lambda} = \{\phi, \Delta, \varepsilon\}$ enter the calculation: The internal constraints, i.e. the properties of the inclusion ϕ and Δ, affect the dynamic operator (and thus its eigenvalues) directly, while the external constraint ε enters by restricting the allowed configurations over which the thermal average is performed. Explicitly, the partition function is given by the functional integral

$$Z = \int \mathcal{D}w \, e^{-\beta \langle w | \mathfrak{D}(\mathbf{\Lambda}) | w \rangle} \Theta(\varepsilon - w(L)) , \qquad (5)$$

where $\beta \equiv (k_B T)^{-1}$, k_B is Boltzman's constant and Θ is Heaviside's step function. Note that in the discrete theory $w(L) = w_N$. We will demonstrate in what follows that these two ways differ drastically in the continuum limit.

The integral in Eq. (5) can be explicitly performed [22], demonstrating that the free energy is composed of two additive contributions,

$$F(\mathbf{\Lambda}) \equiv -k_B T \log Z = F_i(\phi, \Delta) + F_\varepsilon(\mathbf{\Lambda}) . \qquad (6)$$

F_i, which is independent of ε, is the contribution associated with the inclusion parameters and F_ε, that depends also on ϕ and Δ, is the contribution associated with the external constraint ε.

We first consider F_i (corresponding to $F(\varepsilon \to \infty)$). In this case the integral in Eq. (5) is purely quadratic, leading to the following free energy [22]

$$F_i = \frac{k_B T}{2} \log \left[\frac{\det \mathfrak{D}}{(k_B T)^N} \right] = \frac{k_B T}{2} \sum_q \log \left(\frac{\lambda_q}{k_B T} \right) , \quad (7)$$

where λ_q is the eigenvalue associated with the wavenumber q. Thus, the calculation reduces to finding the eigenmodes of $\mathfrak{D}$. While this can be done by fairly standard

methods, we nonetheless sketch the process briefly here, as some of its details will prove crucial to the analysis. The complete calculation is given in [22].

The process is similar to that of calculation of transmission/reflection coefficients in the presence of a square barrier in wave theory or quantum mechanics and its crux lies in the fact that $\kappa(x)$ is locally constant, except for two discontinuity points. Consequently, an eigenmode of $\mathfrak{D}$ must *locally* be a sinusoidal function (or more generally, an eigenmode of the corresponding translationally invariant operator). That is, an eigenmode w_q is of the general form

$$w_q = \begin{cases} \Re\left[A_1 \exp(iqx)\right] & 0 < x < x_1 \\ \Re\left[A_2 \exp(i\tilde{q}x)\right] & x_1 < x < x_2 \ , \\ \Re\left[A_3 \exp(iqx)\right] & x_2 < x < L \end{cases} \qquad (8)$$

where A_i are yet undetermined complex amplitudes and q ($\tilde{q}$) is the wavenumber in the hard (soft) region. The dispersion relation, i.e. the relationship between λ_q and q, differ between the two theories. Explicitly, we have $\lambda_q^{\mathrm{SFT}} = L\kappa_h\, q^2$ and $\lambda_q^{\mathrm{DT}} = 4L\kappa_h(\Delta x)^{-2}\sin^2(q\,\Delta x/2)$. Thus, in order for the eigenvalue equation $\mathfrak{D}\,w_q = \lambda_q\, w_q$ to be satisfied with the same eigenvalue in all regions, we must demand

$$\kappa_h\, q^2 = \kappa_s\, \tilde{q}^2 \qquad \text{(SFT)}\ , \qquad (9)$$

$$\kappa_h \sin^2\left(\frac{q\,\Delta x}{2}\right) = \kappa_s \sin^2\left(\frac{\tilde{q}\,\Delta x}{2}\right) \qquad \text{(DT)}\ . \qquad (10)$$

For the former this reads $\tilde{q} = \Delta\, q$, which is also the case for the latter in the small q limit.

For the continuum operator, the amplitudes A_i are obtained by imposing 6 boundary conditions. There are 2 boundary conditions at the external boundaries $x = 0$ and $x = L$, and additionally, 2 internal boundary conditions at the discontinuity points x_1 and x_2. These correspond to requiring the continuity of $w(x)$ and of the force, i.e. of $\kappa(x)\,w'(x)$ (which implies a discontinuity of $w'(x)$, cf. Fig. 2). Thus, we have 6 homogeneous equations for the 6 amplitudes, and requiring a simultaneous solution translates to a transcendental equation for q (see full derivation in [22]). The set of wavenumbers $\{q_n\}_{n=1}^N$ form the spectrum. In addition, the spectrum of $\boldsymbol{H}$ is calculated numerically (though $\det \mathfrak{D} = \det \boldsymbol{H}$ in Eq. (7) is calculated analytically, see below).

The spectra and 3 selected modes of both operators $\mathfrak{L}$ and $\boldsymbol{H}$ are plotted in Fig. 2. As expected, the two theories agree on the detailed structure of the modes, as well as on the shape of the spectra, in the small-q limit. This agreement, however, prevails only for a small fraction of the modes and there are qualitative discrepancies at higher q, as is evident from the figure.

It is furthermore observed the spectrum of the continuum operator $\mathfrak{L}$ is linear, i.e. the nth wavenumber is given by $q_n = C\,n/L$. The value of C is easily obtained from the transcendental equation that defines the allowed q's, and it can be shown that $C = \pi/(\phi\Delta + 1 - \phi)$ [22]. In
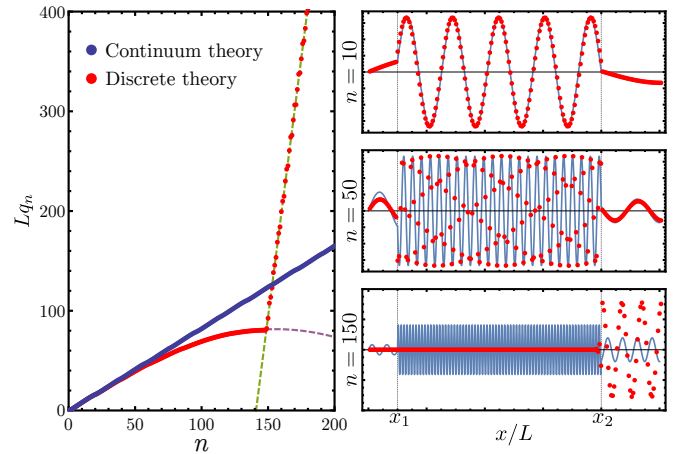

FIG. 2. Left: Spectra of the continuum operator $\mathfrak{L}$ (blue) and the discrete one $\boldsymbol{H}$ (red). The plot shows the nth wavenumber q_n as a function of the ordinal number n for both theories. The dashed lines show a sinusoidal dependences (purple) and a straight line (green). The spectrum of $\boldsymbol{H}$ follows the same linear trend up to $n = 200$, which is not shown here. Right: 3 selected modes of both theories (same color code) from various parts of the spectra (the ordinal number is specified for each panel). The parameters used are $N = 200$, $\Delta = 5$, $x_1/L = 0.1$ and $x_2/L = 0.8$.

sharp contrast, the spectrum of $\boldsymbol{H}$ features a more complicated structure, consisting of two distinct regimes, one is a pure sinusoidal function, and the other is a straight line. The latter is composed of modes that are localized in the right hard region, like the 150th mode shown in Fig. 2. This happens because the condition of Eq. (10) produces an imaginary wavenumber in the soft region, i.e. an evanescent wave. It is seen that a significant fraction of the modes are evanescent in the soft region, and comparing Eq. (9) to Eq. (10) shows that such modes do not exist in the continuum theory, i.e. such evanescent modes do not have a continuum counterpart.

We are now in a position to calculate F_i in both theories according to Eq. (7). Since we have an explicit expression of all the eigenvalues of $\mathfrak{L}$, F^{SFT} is readily calculable and in the large-N limit it takes the form [22]

$$F_i^{\mathrm{SFT}} = Nk_BT \ \times \qquad\qquad (11)$$
$$\left[\tfrac{1}{2}\log\left(\frac{\beta\kappa_h}{L/N}\right) - \log\left(\phi\Delta + 1 - \phi\right) + \log\left(\frac{\sqrt{N}\pi}{e}\right)\right]\ .$$

Using some linear algebraic manipulations on $\boldsymbol{H}$, one obtains $\det \boldsymbol{H} = (\Delta x)^{-N}\prod_i \kappa_i$ [22], which can be used to calculate F^{DT}

$$F_i^{\mathrm{DT}} = Nk_BT\left[\tfrac{1}{2}\log\left(\frac{\beta\kappa_h}{L/N}\right) - \phi\log\Delta\right]\ . \qquad (12)$$

Both Eqs. (11)-(12) were corroborated against explicit numerical calculations [22].

F_i^{SFT} and F_i^{DT} are composed of two contributions, a homogeneous one which does not depend on the inclusion parameters, and an inhomogeneous one which does.

The homogeneous contribution is identical up to a logarithmic factor in N, a common situation in SFT calculations [3]. The inhomogeneous contribution, however, has a fundamentally different form.

The contribution of the inhomogeneity to the fluctuation-induced force, $\chi_\phi \equiv \partial F_i / \partial \phi$, takes the form

$$\chi_\phi^{\text{SFT}} = -Nk_BT\frac{\Delta - 1}{(\Delta - 1)\phi + 1} \ , \tag{13}$$

$$\chi_\phi^{\text{DT}} = -Nk_BT\log\Delta \ , \tag{14}$$

in the SFT and DT, respectively. Physically, it corresponds — e.g. in the case of cofilin-mediated softening of actin filaments (where local softening of the actin polymer is induced by the adsorption of cofilin molecules from the solvent [18]) — to the fluctuation-induced contribution to an adsorption force. The latter also includes other contributions, e.g. a binding energy, the change in the solvent mixing entropy and the entropy associated with placing the inclusion at different locations along the polymer, which are of no interest in the present context. Finally, below we show that $\partial F_\varepsilon / \partial \phi$ is identical in both theories.

Equations (13)-(14) are the main results of this Letter. The two results are qualitatively different (except for the small contrast limit $\Delta \to 1$, where $\chi_\phi^{\text{SFT}} \approx \chi_\phi^{\text{DT}} \sim \Delta - 1$), demonstrating fundamental discrepancies between the continuum and discrete theories in this case. In particular, χ_ϕ^{DT} is independent of ϕ, while χ_ϕ^{SFT} depends on it. Similar discrepancies are observed when the variation of the free energies with respect to Δ is considered. We stress that these discrepancies are not mitigated when the discretization length is taken to zero, when a different ultra-violet cutoff is used or when the variation of $\kappa(x)$ is smoothed out [22]. We interpret this as an example for the breakdown of the continuum theory of inhomogeneous systems.

It is worthwhile restating the origin of this breakdown. Since the contribution of an eigenmode to the sum in Eq. (7) increases as $\log(\lambda_q)$, and since the spectra of the two theories differ substantially in the high-q regime, the two theories produce different predictions. That is, when the inclusion parameters ϕ and Δ are varied, not only the identical small-q properties of the continuum and discrete spectra vary, rather the *entire* spectra — which are manifestly different — vary.

Next we consider F_ε in Eq. (6). The calculation of the partition function in the presence of a finite external constraint ε is somewhat more involved, yet it is still completely tractable and takes the form [22]

$$F_\varepsilon = k_BT\log\left[1 + \text{erf}\left(\varepsilon\sqrt{\frac{\beta\kappa_h}{\ell(\phi,\Delta)}}\right)\right] \ ,$$
$$\text{with } \ell(\phi,\Delta) \propto \sum_q \frac{w_q(L)^2}{\lambda_q} \ , \tag{15}$$

valid for *both* SFT and DT. Here erf is the error function and ℓ is a length scale that depends on the inclusion parameters through the properties of the eigenmodes w_q and the eigenvalues λ_q.

What can be said about the thermodynamic force on the wall, $\chi_\varepsilon \equiv \partial F_\varepsilon / \partial \varepsilon$? Does it exhibit similar discrepancies between the theories as in Eqs. (13)-(14)? Since the two theories feature the same functional form of F_ε, all of the interesting physics is encapsulated in the length scale $\ell(\phi,\Delta)$. However, as opposed to F_i, where the contribution of the different modes increases with increasing q, the sum that defines ℓ is dominated by small-q contributions because $w_q(L)/\lambda_q$ is a strongly decaying function of q. That is, we expect $\ell(\phi,\Delta)$ to mainly depend on the small-q part of the spectrum, for which the two theories coincide. This is supported by an explicit calculation [22], hence we conclude that $\chi_\varepsilon^{\text{SFT}} = \chi_\varepsilon^{\text{DT}}$ in the thermodynamic limit and that the continuum theory is valid in this case.

In summary, the analysis revealed qualitative differences between the continuum and discrete calculations of certain Casimir-like forces, which arise from the variation of the free energy with respect to some — but not necessarily all — macroscopic symmetry-breaking parameters Λ. One may then ask whether it is possible to modify the continuum theory, e.g. in the spirit of Debye's theory of the heat capacity of homogeneous systems (where the continuum dispersion relation is used along with a cutoff that ensures that the total number of modes agrees with the discrete theory), to better agree with the discrete one. While we cannot entirely exclude this possibility, we have not yet found a way to do so.

Our results might have implications for a broader class of fluctuation-induced (Casimir-like) force calculations, which a priori invoke the continuum approximation. While the physical problem we solved may differ in some aspects from various continuum fluctuation-induced force calculations (where the latter may involve higher dimensionality and inclusions of fixed sizes at variable locations/orientations), our results at least indicate that the continuum approximation/assumption in this context should be carefully reexamined.

[1] M. Kardar, *Statistical physics of fields* (Cambridge University Press, Cambridge, 2007).

[2] A. Altland and B. D. Simons, *Condensed Matter Field Theory*, 2nd ed. (Cambridge University Press, Cambridge, 2010).

[3] S. A. Safran, *Statistical thermodynamics of surfaces, interfaces, and membranes* (Addison-Wesley, 1994).

[4] P. Chaikin and T. C. Lubensky, *Principles of condensed matter physics* (Cambridge University Press, Cambridge, 1995).

[5] M. Goulian, R. Bruinsma, and P. Pincus, Europhys. Lett. **22**, 145 (1993).

[6] R. Golestanian, M. Goulian, and M. Kardar, Phys. Rev. E **54**, 6725 (1996).

[7] H.-K. Lin, R. Zandi, U. Mohideen, and L. P. Pryadko, Phys. Rev. Lett. **107**, 228104 (2011).

[8] H. Li and M. Kardar, Phys. Rev. Lett. **67**, 3275 (1991).

[9] H. Li and M. Kardar, Phys. Rev. A **46**, 6490 (1992).

[10] H. Lehle and M. Oettel, Phys. Rev. E **75**, 011602 (2007).

[11] T. C. Halsey and W. Toor, J. Stat. Phys. **61**, 1257 (1990).

[12] R. Bruinsma, M. Goulian, and P. Pincus, Biophys. J. **67**, 746 (1994).

[13] A. Ajdari, L. Peliti, and J. Prost, Phys. Rev. Lett. **66**, 1481 (1991).

[14] D. R. Nelson and P. Le Doussal, Phys. Rev. B **42**, 10113 (1990).

[15] M. Paczuski, M. Kardar, and D. R. Nelson, Phys. Rev. Lett. **60**, 2638 (1988).

[16] D. Nelson, T. Piran, and S. Weinberg, *Statistical mechanics of membranes and surfaces* (World Scientific, 2004).

[17] E. Prochniewicz, N. Janson, D. D. Thomas, and E. M. De la Cruz, J. Mol. Biol. **353**, 990 (2005).

[18] B. R. McCullough, L. Blanchoin, J.-L. Martiel, and E. M. De La Cruz, J. Mol. Biol. **381**, 550 (2008).

[19] O. N. Yogurtcu, J. S. Kim, and S. X. Sun, Biophys. J. **103**, 719 (2012).

[20] V. E. Galkin, A. Orlova, D. S. Kudryashov, A. Solodukhin, E. Reisler, G. F. Schröder, and E. H. Egelman, Proc. Natl. Acad. Sci. U. S. A. **108**, 20568 (2011).

[21] G. B. Arfken, *Mathematical methods for physicists*, 4th ed. (Academic press, 2013) p. 539.

[22] Supplementary material is appended at the end of this file.

Supplemental Materials for:
"Breakdown of statistical field theory of inhomogeneous polymers"

This document is meant to provide additional technical details related to results reported on in the manuscript.

I. DETAILS OF CONTINUUM ANALYSIS

Consider a general one-dimensional system whose energy is treated to quadratic order. The continuum energy takes the form

$$U^{\text{SFT}}(w(x)) = \frac{1}{2} \langle w(x)|\mathfrak{L}|w(x)\rangle \equiv \frac{1}{2L} \int_0^L w(x)\, \mathfrak{L}\, w(x)\, dx \ ,$$

where $\mathfrak{L}$ is a self-adjoint real differential operator. Our convention is that the eigenvalues of $\mathfrak{L}$ are of energy dimensions, and thus $w(x)$ is dimensionless. For the system discussed in the main text we have

$$\mathfrak{L}\{w(x)\} = -L\frac{\partial}{\partial x}\left(\kappa(x)\frac{\partial w}{\partial x}\right) \ . \tag{S1}$$

We will work in the eigenbasis of $\mathfrak{L}$, which we denote by $w_{q_1}(x), \ldots, w_{q_N}(x)$. These function are orthonormal, i.e.

$$\frac{1}{L}\int_0^L w_q w_{q'} dx = \delta_{qq'} \quad \text{and} \quad \langle w_q|\mathfrak{L}|w_{q'}\rangle = \lambda_q \delta_{qq'} \ , \tag{S2}$$

where λ_q is the eigenvalue associated with w_q. The eigenmodes span the functional space and a general configuration $w(x)$ can be written as $w(x) = \sum a_q w_q(x)$ where $a_q \equiv \langle w(x)|w_q\rangle$. The energy is thus written as $U^{\text{SFT}} = \frac{1}{2}\sum_q \lambda_q a_q^2$, and the partition function is

$$Z^{\text{SFT}} = \int \mathfrak{D}w\, e^{-\beta\langle w|\mathfrak{L}|w\rangle}\Theta\Big(\varepsilon - w(L)\Big) \tag{S3}$$

$$= \int d^N a_q \exp\left[-\beta\sum_q \tfrac{1}{2}\lambda_q a_q^2\right]\Theta\Big(\varepsilon - \sum_q a_q w_q(L)\Big) \ .$$

This is a multivariate Gaussian integral over a half-space. In Sec. V we calculate a general formula for integrals of this type. Applying this formula (Eq. (S37)) to Eq. (S3) yields

$$Z^{\text{SFT}} = \frac{1}{2}\left(\frac{(2\pi)^N}{\beta^N \det \mathfrak{L}}\right)^{1/2}\left(1 + \text{erf}\left[\varepsilon\sqrt{\frac{\beta\kappa_h}{\ell^{\text{SFT}}}}\right]\right) \tag{S4}$$

$$\ell^{\text{SFT}} \equiv 2L\sum_q \left(\frac{w_q(L)}{qL}\right)^2 \ . \tag{S5}$$

where erf is the standard error function and the relation $\lambda_q = \kappa_h L q^2$ was used. $\det \mathfrak{L}$ is defined as $\prod_q \lambda_q$. The factor $\frac{1}{2}(2\pi)^{N/2}$ is of no physical importance and will be omitted in what follows.

Note that here we take into account exactly N continuum modes, which is basically a choice of an ultraviolet cutoff on q. The results presented here do not depend qualitatively on the choice of the ultraviolet cutoff, as long as the number of modes scales with N, which is anyway a trivial requirement from any reasonable cutoff scheme.

The free energy is thus given by

$$F^{\text{SFT}} \equiv -k_B T \log Z^{\text{SFT}} = F_i^{\text{SFT}} + F_\varepsilon^{\text{SFT}} \ ,$$

$$F_i^{\text{SFT}} \equiv \tfrac{1}{2}k_B T \log\left(\beta^N \det \mathfrak{L}\right) \ , \tag{S6}$$

$$F_\varepsilon^{\text{SFT}} \equiv -\tfrac{1}{2}k_B T \log\left(1 + \text{erf}\left[\varepsilon\sqrt{\frac{\beta\kappa_h}{\ell^{\text{SFT}}}}\right]\right) \ .$$

We now turn to calculate $\det \mathfrak{L}$, which is done by explicit calculation of the eigenmodes.

A. General form of the eigenmodes

The calculation is very much in the spirit of standard wave theory analysis of reflection and refraction from a sharp material boundary, or of quantum mechanical treatment of transmission over a potential barrier step. The operator of interest is defined in Eq. (S1) and its eigenmodes can be found by solving the continuum eigenvalue equation,

$$\mathfrak{L}w(x) = \lambda w(x) \ , \tag{S7}$$

which in general is a non-trivial task. However, since $\kappa(x)$ is locally constant for $x \neq x_1, x_2$, treating the soft and hard polymeric segments separately significantly simplifies the mathematical structure. That is, in each segment separately κ is space-independent, so Eq. (S7) reads

$$\kappa(x)\, w_q''(x) = \lambda_q^{\text{SFT}}\, w_q(x) \ . \tag{S8}$$

It is thus natural to write the solution separately for the different segments. For each segment, we write $w_q(x)$ as a superposition of the two independent solutions of Eq. (S8) in the form

$$w_q(x) = \begin{cases} A_1\cos(qx) + A_2\sin(qx) & 0 < x < x_1 \\ A_3\cos(\tilde{q}x) + A_4\sin(\tilde{q}x) & x_1 < x < x_2 \\ A_5\cos(qx) + A_6\sin(qx) & x_2 < x < L \end{cases} ,$$

where the A_i are yet undetermined real amplitudes (note that in Eq. (8) of the main text a complex notation was used). We also impose the supplementary condition

$$q^2\kappa_h = \tilde{q}^2\kappa_s \ , \tag{S9}$$

which ensures that Eq. (S8) is satisfied with the *same* eigenvalue $\lambda_q^{\text{SFT}} = L\kappa_h q^2 = L\kappa_s \tilde{q}^2$ at all points in space. A mode with negative q can be obtained by rearranging the coefficients $\{A_i\}$ in the corresponding mode with a positive q, so we only consider modes with $q > 0$.
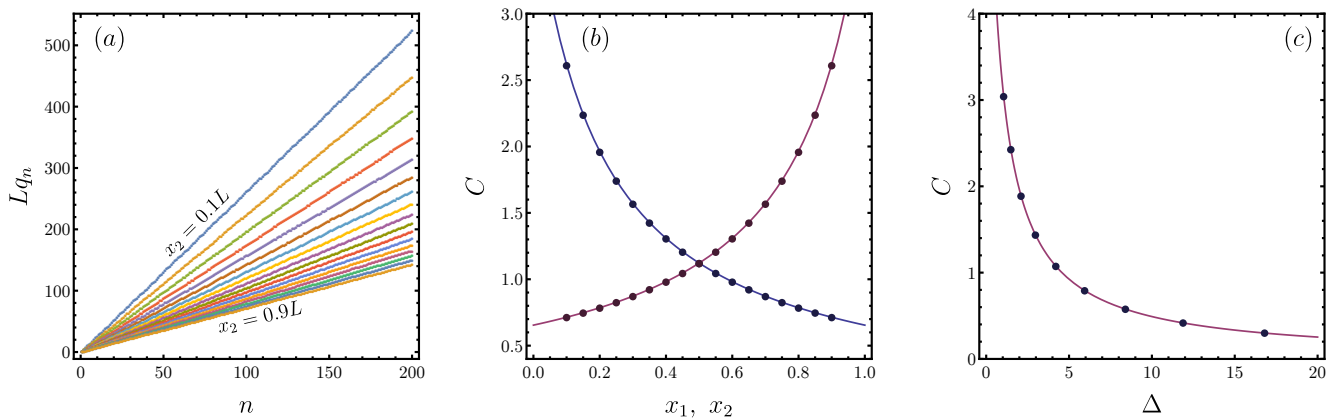
FIG. S1. **(a)** The numerically found q's as a function of their ordinal number for fixed $x_1 = 0.05L$ and $\Delta = 5$. Different colors correspond to different values of x_2 which varies at constant steps between $0.1L$ and $0.9L$. **(b)** The blue points show the slopes of the data in panel (a) as a function of x_2, and the solid line is the prediction Eq. (S16). The purple data are obtained with the same procedure, but when $x_2 = 0.95L$ is fixed and x_1 varies. **(c)** The same as (b), but now Δ is varied and $x_1 = 0.2L$, $x_2 = 0.8L$ are fixed.

B. Boundary conditions

The 6 amplitudes are determined by 6 boundary conditions (BC). 2 boundary conditions are given at the external boundaries $x = 0$ and $x = L$, and 2 more are imposed on each of the internal boundaries x_1 and x_2. Here we derive these internal boundary conditions.

The spatiotemporal dynamics of the system are governed by the equation

$$\mathcal{T}\{w(x,t)\} = \mathfrak{L}\{w(x,t)\} \, , \qquad (S10)$$

where $\mathcal{T}$ is a differential operator acting on the time coordinate. $\mathcal{T}\{w(x,t)\}$ is proportional to $\partial_{tt}w(x,t)$ in inertial systems, to $\partial_t w(x,t)$ in highly overdamped systems and might have a more complicated structure in other cases. Since the particular form of $\mathcal{T}$ is irrelevant to this discussion, we do not specify it here. We integrate Eq. (S10) over a region of size δ around the a discontinuity point, say x_1. That is, we consider the region $-\delta < x - x_1 < \delta$ and take the limit $\delta \to 0$. Using the fact that for $x \neq x_1$ κ is space-independent, the integration yields

$$
\lim_{\delta \to 0} \frac{1}{L} \int_{x_1-\delta}^{x_1+\delta} \mathcal{T}\{w(x,t)\}dx = \\
\lim_{\delta \to 0} \left[\kappa_s \, w'|_{x=\delta} - \kappa_h \, w'|_{x=-\delta} \right] \, . \qquad (S11)
$$

Irrespective of the explicit form of $\mathcal{T}$, we know that it does not produce a singularity at $x = x_1$ and thus the left-

hand-side of the above equation vanishes. We therefore conclude that the function $\kappa(x)\,w'(x)$ is continuous across the interface.

Integrating Eq. (S10) and dividing by $\kappa(x)$ we obtain

$$\frac{1}{L\,\kappa(x)} \int \mathcal{T}\{w(x,t)\}dx = w'(x,t) \, . \qquad (S12)$$

Integrating again over the interval $[x_1 - \delta, x_1 + \delta]$ and taking the limit $\delta \to 0$, the left-hand-side vanishes and we see that $w(x)$ is continuous across $x = x_1$. As before, we use the fact that although κ is discontinuous, it is not singular and the integral of it over a vanishingly small region vanishes.

To summarize, the 6 boundary conditions are

$$w(0) = w'(L) = [\![w]\!]_{x_1} = [\![w]\!]_{x_2} = [\![\kappa w']\!]_{x_1} = [\![\kappa w']\!]_{x_2} = 0 \, ,$$

where $[\![\cdot]\!]_{x_i}$ denotes the jump in a given quantity at $x = x_i$. In particular, as $\kappa(x)$ is discontinuous at x_1 and x_2, $w'(x)$ experiences a jump-discontinuity at these points. The somewhat formal derivation of the internal BC at x_1 and x_2 presented above has a clear physical meaning that could have been invoked a priori; at any discontinuity of the linear elastic modulus κ, the polymer retains its integrity, i.e. $w(x)$ is continuous, and the stress (either torsional or extensional) is continuous, i.e. $\kappa(x)\,w'(x)$ is continuous.

The BC can be summarized concisely in the matrix equation

$$
\begin{pmatrix}
1 & 0 & 0 & 0 & 0 & 0 \\
0 & 0 & 0 & 0 & -\sin(Lq) & \cos(Lq) \\
\cos(qx_1) & \sin(qx_1) & -\cos(\Delta qx_1) & -\sin(\Delta qx_1) & 0 & 0 \\
-\Delta \sin(qx_1) & \Delta \cos(qx_1) & \sin(\Delta qx_1) & -\cos(\Delta qx_1) & 0 & 0 \\
0 & 0 & \cos(\Delta qx_2) & \sin(\Delta qx_2) & -\cos(qx_2) & -\sin(qx_2) \\
0 & 0 & \sin(\Delta qx_2) & -\cos(\Delta qx_2) & -\Delta \sin(qx_2) & \Delta \cos(qx_2)
\end{pmatrix}
\begin{pmatrix}
A_1 \\ A_2 \\ A_3 \\ A_4 \\ A_5 \\ A_6
\end{pmatrix} = 0 \, . \qquad (S13)
$$

C. The constant $C(\Delta, x_1, x_2)$

In order to satisfy the boundary conditions simultaneously, the determinant of the matrix must vanish. The resulting equation can be solved numerically to find the discrete set of permissible q's. The eigenvectors are easily found by calculating the kernel of the matrix, together with the normalization condition (S2). Explicitly, the demand that the determinant vanish reads

$$
\begin{aligned}
0 = \; & \left(\tfrac{\Delta+1}{\Delta-1}\right)^2 \cos\left[q((x_2 - x_1)(\Delta - 1) + L)\right] \\
& + \tfrac{\Delta+1}{\Delta-1} \cos\left[q((x_2 - x_1)\Delta - (x_2 + x_1) + L)\right] \\
& - \tfrac{\Delta+1}{\Delta-1} \cos\left[q(-(x_2 - x_1)\Delta - (x_2 + x_1) + L)\right] \\
& - \cos\left[q((x_1 - x_2)(1 + \Delta) + L)\right] .
\end{aligned} \tag{S14}
$$

The problem now is to estimate how the permissible q's are distributed as a function of the parameters. To this end, we numerically solve Eq. (S14) for some range of inclusion parameters. In Fig. S1 we plot the numerically found q's as a function of their ordinal number, when we fix x_1 and Δ, and x_2 is varied. It is seen that the spectrum is linear, i.e. that one can write the n-th wave number as

$$
q_n = \frac{C(\Delta, x_1, x_2)}{L} n . \tag{S15}
$$

Simple dimensional analysis of Eq. (S14) shows that C cannot depend on L nor on κ_h or κ_s, except through their ratio Δ^2.

How can we calculate $C(\Delta, x_1, x_2)$? The defining equation, Eq. (S14), is a sum of sinusoidal functions with different frequencies. One can conjecture that the highest frequency, $(\Delta - 1)(x_2 - x_1) + L$, is the one that controls the density of solutions to Eq. (S14). This argument predicts that the equation for C should read

$$
C = \frac{\pi L}{(\Delta - 1)(x_2 - x_1) + L} = \frac{\pi}{\phi\Delta + 1 - \phi} . \tag{S16}
$$

Fig. S1 demonstrates a numerical verification of this prediction.

D. Calculating the free energy

With the wavenumbers at hand, i.e. Eqs. (S15)-(S16), the calculation of F^{SFT} is straightforward. The eigenvalue associated with the wavenumber q is $\lambda_q^{\text{SFT}} = L\,\kappa_h\,q^2$ and thus

$$
\det \mathfrak{L} = \prod_q \lambda_q^{\text{SFT}} = \prod_n \kappa_h L q_n^2 = \left(\frac{\kappa_h}{L}\right)^N C^{2N}(N!)^2 .
$$

This immediately leads to

$$
F^{\text{SFT}} = \frac{1}{2} k_B T \log\left[\beta^N \det \mathfrak{L}\right] = \tag{S17}
$$

$$
Nk_B T \left[\tfrac{1}{2}\log\left(\frac{\beta\kappa_h}{L}\right) - \log\left(\frac{\phi\Delta + 1 - \phi}{\pi}\right) + \frac{1}{N}\log N!\right].
$$

We now apply Stirling's approximation, which we write as $\log(N!) \approx N \log\left(\frac{N}{e}\right)$ to obtain

$$
\begin{aligned}
F^{\text{SFT}} \approx Nk_B T \Big[& \tfrac{1}{2}\log\left(\frac{\beta\kappa_h}{L}\right) \\
& - \log(\Delta\phi + 1 - \phi) + \log\left(N\frac{\pi}{e}\right) \Big] .
\end{aligned} \tag{S18}
$$

After minor rearrangement, Eq. (11) of the main text is recovered.

II. DETAILS OF DISCRETE ANALYSIS

We want to calculate the partition function

$$
Z^{\text{DT}} = \int_{-\infty}^{\infty} d^N \boldsymbol{w}\, e^{-\beta U^{\text{DT}}(\boldsymbol{w})} \Theta(\varepsilon - w_N) , \tag{S19}
$$

with

$$
U^{\text{DT}}(\boldsymbol{w}) = \sum_{i=1}^N \frac{1}{2}\kappa_i \left(\frac{w_i - w_{i-1}}{\Delta x}\right)^2 \Delta x . \tag{S20}
$$

Unlike the continuum case described in the previous section, here the calculation can be performed without explicit reference to the eigenmodes. The trick is to use the non-orthogonal change of variables

$$
y_i \equiv \sqrt{\frac{\kappa_i}{\Delta x}}(w_i - w_{i-1}) , \quad w_i = \sum_{j=1}^i y_j \sqrt{\frac{\Delta x}{\kappa_j}} . \tag{S21}
$$

The Jacobian of this transformation is $\prod_i \sqrt{\frac{\kappa_i}{\Delta x}} = \sqrt{\det \boldsymbol{H}}$. With the new variables y_i the energy takes the simple form $U = \frac{1}{2}||\boldsymbol{y}||^2$. The partition function is thus

$$
Z^{\text{DT}} = \sqrt{\frac{1}{\det \boldsymbol{H}}} \int_{-\infty}^{\infty} d^N \boldsymbol{y}\, e^{-\frac{\beta}{2}|\boldsymbol{y}|^2} \Theta\left(\varepsilon - \sum_j y_j \sqrt{\frac{\Delta x}{\kappa_j}}\right) .
$$

This is an Gaussian integral over a half-space, for which we develop an explicit formula in Sec. V. The result is

$$
Z^{\text{DT}} = \frac{1}{2}\sqrt{\frac{(2\pi)^N}{\beta^N \det \boldsymbol{H}}} \left(1 + \text{erf}\left[\varepsilon\sqrt{\frac{\beta\kappa_{\text{eff}}}{2\Delta x}}\right]\right) , \tag{S22}
$$

where we introduced the notation $\kappa_{\text{eff}} \equiv \left(\sum \kappa_i^{-1}\right)^{-1}$, i.e. the effective spring constant of the chain.

This expression holds for an arbitrary choice of κ_i. If we assume $\kappa(x)$ has the form described in the main text, i.e. $N\phi$ springs have a spring constant of κ_s and $N(1-\phi)$ have a spring constant of κ_h, we have

$$
\kappa_{\text{eff}} = \left(\frac{N\phi}{\kappa_s} + \frac{N(1-\phi)}{\kappa_h}\right)^{-1} = \frac{\kappa_h/N}{\Delta^2\phi + (1-\phi)} \tag{S23}
$$

$$
\det \boldsymbol{H} = \prod_i \frac{\kappa_i}{\Delta x} = \left(\frac{\kappa_h}{\Delta x}\right)^N \Delta^{-2N\phi} \tag{S24}
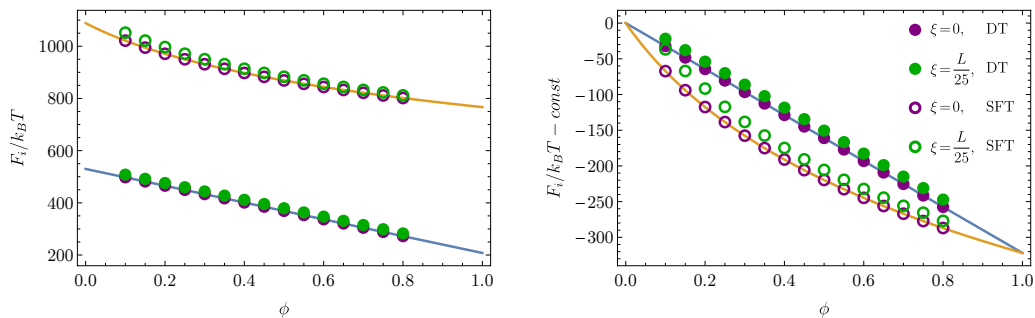$$

FIG. S2. Left: Dependence of the inhomogeneity free-energy F_i on ϕ. Here ϕ was changed by keeping $x_1 = L/10$ and varying x_2. F_i is calculated explicitly by finding the eigenvalues of the operators $\boldsymbol{H}$ (filled symbols) and $\mathfrak{L}$ (empty symbols). Right: for easier comparison, we subtract from each set of data the part which does not depend on the inhomogeneity, i.e. $\frac{N}{2}k_BT\log\left(N\beta\kappa_h/L\right)$, and in addition the factor $\frac{N}{2}k_BT\log\left(N\frac{\pi}{e}\right)$ for the SFT. Green symbols correspond to calculations with smooth $\kappa(x)$, see Sec. IV. The solid lines show the analytic predictions, Eqs. (11)-(12) of the main text.

Thus, the free energy is

$$F^{\mathrm{DT}} \equiv -k_BT\log Z^{\mathrm{DT}} = F_i^{\mathrm{DT}} + F_\varepsilon^{\mathrm{DT}} \ ,$$

$$F_i^{\mathrm{DT}} \equiv \tfrac{1}{2}k_BT\log\left(\beta^N \det\boldsymbol{H}\right)$$

$$= \frac{N}{2}k_BT\left[\log\left(\frac{\beta\kappa_h}{L/N}\right) - \phi\log\Delta\right] \ , \qquad (\mathrm{S25})$$

$$F_\varepsilon^{\mathrm{SFT}} \equiv -\tfrac{1}{2}k_BT\log\left(1 + \mathrm{erf}\left[\varepsilon\sqrt{\frac{\beta\kappa_h}{\ell^{\mathrm{DT}}}}\right]\right)$$

$$\ell^{\mathrm{DT}} = 2L\left(\Delta^2\phi + (1-\phi)\right) \ . \qquad (\mathrm{S26})$$

III. NUMERICAL VERIFICATION

All the analytic predictions presented here and in the main text were verified against direct numerical calculations. Here we present a few of the comparisons, all of which show perfect agreement.

The numerical and analytic predictions for the inhomogeneity contribution to the free energy, F_i, is shown in Fig. S2.

In Fig. S3 we test the analytic predictions for ℓ^{DT} and ℓ^{SFT}. In addition to the agreement with the numerics we show also that the sum that defines ℓ^{SFT}, Eq. (S5), converges to the analytic prediction for ℓ^{DT}, Eq. (S26), after summing over a sub-extensive number of modes. To show this, we define ℓ_k^{SFT} as the partial sum of Eq. (S5) over the first k modes,

$$\ell_k^{\mathrm{SFT}} \equiv 2L\sum_{i=1}^{k}\left(\frac{w_{q_i}(L)}{q_iL}\right)^2 \ . \qquad (\mathrm{S27})$$

Note that $\ell_N^{\mathrm{SFT}} = \ell^{\mathrm{SFT}}$, and in Fig. S3 we show that ℓ_k^{SFT} with $k > 10$ is already close to ℓ^{DT} to within 1%.
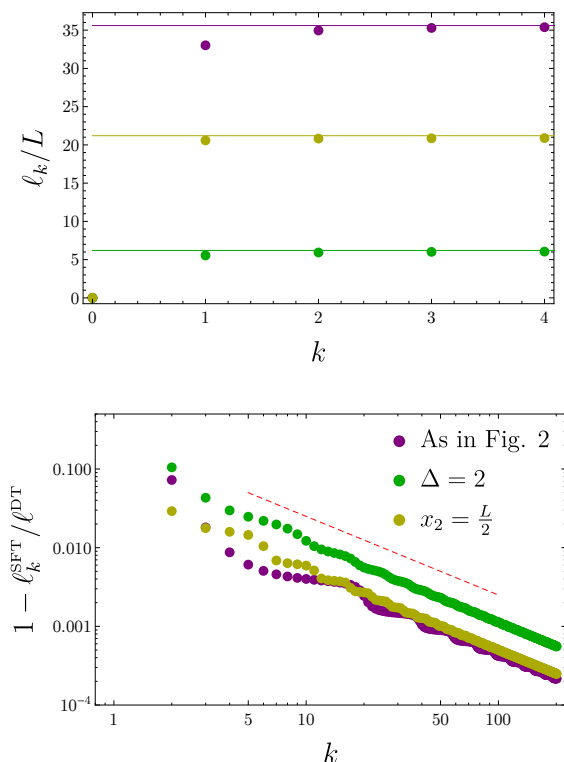
FIG. S3. Top: Convergence of ℓ_k^{SFT} (cf. Eq. (S27)) to ℓ^{DT}. The purple data use the parameters of Fig. 2 of the main text, and other colors correspond to changing one of the parameters, as described in the legend of the bottom panel. Points correspond to ℓ_k^{SFT} and the lines correspond both to the numerical calculation of ℓ^{DT} and to the analytic prediction, Eq. (S26), which are indistinguishable. It is seen that the results converge after summing over the first few modes. Bottom: The relative error of ℓ_k^{SFT}. It is seen that after summing over the ~ 10 lowest-q modes, ℓ_k^{SFT} already estimates ℓ^{DT} to more than a 1% accuracy for all parameters tested.
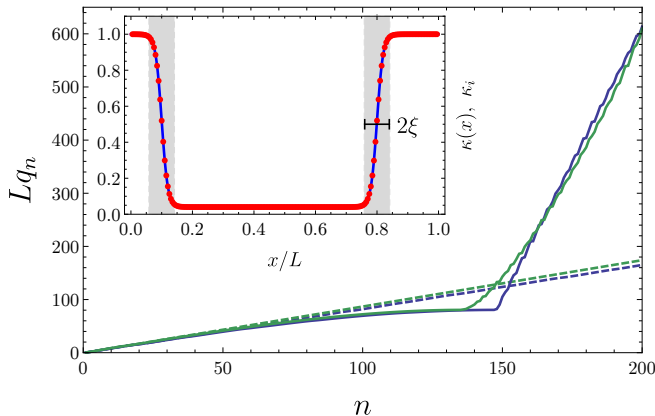
FIG. S4. The spectrum of the SFT operator (dashed lines) and the discrete operator (solid lines) for the case $\ell = L/25$ (green) and $\ell = 0$ (blue) which is discussed in the manuscript. Inset: The smoothed $\kappa(x)$ (solid line) and the discrete κ_i (points). The parameters used are the same as those of Fig. 2 of the main text, together with $\ell = L/25$. The shaded regions, each of width 2ℓ, show the region where κ varies.

IV. SMOOTH VARIATION OF $\kappa(x)$

The continuum eigenmodes of a system with a smoothly varying $\kappa(x)$ can be obtained using a straightforward shooting method. The eigenvalue equation

$$\frac{\partial}{\partial x}\left(\kappa(x)\frac{\partial w}{\partial x}\right) = \lambda\, w(x) \qquad \text{(S28)}$$

is interpreted as a differential equation which is integrated with the initial conditions $w(0)=0$ and $w'(0)=1$. The equation is integrated up to $x = L$ and the value $w'(L;\lambda)$ is obtained as a function of λ. The eigenvalues are those λ for which $w'(L;\lambda)=0$. These are found using standard root-finding methods.

To explore the effect of the smoothness of $\kappa(x)$ on the results, we chose a specific form of smoothing. Instead of a sharp step function, defined as

$$\Theta(x) = \begin{cases} 0 & x < 0 \\ 1 & x > 0 \end{cases}, \qquad \text{(S29)}$$

we use a hyperbolic tangent function that varies over a finite lengthscale ξ

$$\Theta(x;\xi) = \frac{1}{2}\left[1 + \tanh\left(\frac{2x}{\xi}\right)\right]. \qquad \text{(S30)}$$

ξ can be significantly larger than the monomeric lengthscale. Equation (S29) in recovered in the limit $\xi \to 0$. An example of a smoothed $\kappa(x)$ with $\xi = L/25$ is shown in Fig. S4. The computed spectra are also shown and it is seen that the effect of ξ on the spectrum is small and the qualitative discrepancies between the continuum and discrete theories persist. Moreover, the qualitative discrepancies between the continuum and discrete theories are independent of ξ, at least as long as $\xi \ll L$.

V. HALF-SPACE GAUSSIAN INTEGRALS

The partition function, defined in Eq. (5) of the main text, is a multivariate Gaussian integral over a half space. In this section we calculate such an integral in a general manner, to be used in calculations of Z^{DT} and Z^{SFT}.

We want to calculate the integral

$$I(\boldsymbol{A}, \boldsymbol{v}) = \int_{-\infty}^{\infty} d^N\boldsymbol{x}\, e^{-\frac{1}{2}\boldsymbol{x}^T\boldsymbol{A}\boldsymbol{x}}\Theta\left(b - \boldsymbol{v}\cdot\boldsymbol{x}\right). \qquad \text{(S31)}$$

That is, the integral of a multivariate Gaussian over the half space defined by $\boldsymbol{v}\cdot\boldsymbol{x} < b$. $\boldsymbol{v}$ is an arbitrary real vector and $\boldsymbol{A}$ is a strictly positive-definite symmetric matrix. We begin with the simpler case where $\boldsymbol{A}$ is diagonal. The generalization for the non-diagonal case will be immediate. The integral is then

$$I(\boldsymbol{A}, \boldsymbol{v}) = \int_{-\infty}^{\infty} d^N\boldsymbol{x}\, e^{-\frac{1}{2}\sum_i \lambda_i x_i^2}\Theta\left(b - \boldsymbol{v}\cdot\boldsymbol{x}\right),$$

where the λ_i's are the eigenvalues of $\boldsymbol{A}$. We replace the Heaviside function by the integral identity

$$\Theta(b-x) = \int_{-\infty}^{b}\delta(z-x)dz = \int_{-\infty}^{b}\frac{dz}{2\pi}\int_{-\infty}^{\infty}d\omega\, e^{i\omega(z-x)},$$

where two auxiliary variables, ω and z, were introduced. This identity holds for arbitrary $x,b \in \mathbb{R}$. With this replacement, after simple rearrangement the integral is written as

$$I = \int_{-\infty}^{b}\frac{dz}{2\pi}\int_{-\infty}^{\infty}e^{i\omega z} \times \qquad \text{(S32)}$$
$$\left(\prod_{j=1}^{N}\int_{-\infty}^{\infty}dx_j\,\exp\left[-\left(\frac{1}{2}\lambda_j x_j^2 + i\omega v_j x_j\right)\right]\right)d\omega.$$

This is a product of Gaussian integrals, for each of which we can use the integral identity

$$\int_{-\infty}^{\infty}\exp\left[-\frac{1}{2}az^2 \pm i\omega z\right]dz = \sqrt{\frac{2\pi}{a}}e^{-\frac{\omega^2}{2a}}, \qquad \text{(S33)}$$

which holds for any $\omega \in \mathbb{C}$ and real $a > 0$. Thus,

$$I = \int_{-\infty}^{b}\frac{dz}{2\pi}\int_{-\infty}^{\infty}d\omega e^{i\omega z}\prod_{i=1}^{N}\sqrt{\frac{2\pi}{\lambda_i}}e^{-\frac{\omega^2 v_i^2}{2\lambda_i}} \qquad \text{(S34)}$$
$$= \sqrt{\frac{(2\pi)^N}{\det \boldsymbol{A}}}\int_{-\infty}^{b}\frac{dz}{2\pi}\int_{-\infty}^{\infty}d\omega e^{-\frac{1}{2}\left(\sum_i \frac{v_i^2}{\lambda_i}\right)\omega^2 + i\omega b}.$$

The latter is again a Gaussian integral of the form of Eq. (S33), and denoting $D \equiv \sum_i \frac{v_i^2}{\lambda_i} = \boldsymbol{v}^T\boldsymbol{A}^{-1}\boldsymbol{v}$ we get

$$I = \sqrt{\frac{(2\pi)^N}{\det \boldsymbol{A}}}\int_{-\infty}^{b}dz\sqrt{\frac{2\pi}{D}}e^{-\frac{z^2}{2D}}. \qquad \text{(S35)}$$

The last integral is expressed in terms of the standard error function

$$\text{erf}(z) \equiv \frac{2}{\sqrt{\pi}} \int_0^z e^{-x^2} dx \ , \qquad (\text{S36})$$

such that

$$I(\boldsymbol{A}, \boldsymbol{v}) = \frac{1}{2} \sqrt{\frac{(2\pi)^N}{\det \boldsymbol{A}}} \left[1 + \text{erf}\left(\frac{b}{\sqrt{2D}}\right) \right] \ , \qquad (\text{S37})$$
$$D \equiv \boldsymbol{v}^T \boldsymbol{A}^{-1} \boldsymbol{v} \ .$$

This completes the derivation. While this is not necessary for the present needs, we note that the formula (S37) is valid also when $\boldsymbol{A}$ is not diagonal. This can be seen by a simple change of variables.